ORIGINAL ARTICLE

Koch's Triangle and the Atrioventricular Node in Ebstein's Anomaly: Implications for Catheter Ablation

Damián Sánchez-Quintana,[a] Beatriz Picazo-Angelín,[b] Alberto Cabrera,[c] Margarita Murillo,[a] and José Ángel Cabrera[d]

[a]Departamento de Anatomía y Biología Celular, Universidad de Extremadura, Facultad de Medicina, Badajoz, Spain
[b]Servicio de Pediatría, Hospital Costa del Sol, Marbella, Málaga, Spain
[c]Servicio de Pediatría, Hospital Cruces de Baracaldo, Bilbao, Spain
[d]Unidad de Arritmias, Departamento de Cardiología, Hospital-Quirón Madrid, Universidad Europea de Madrid, Madrid, Spain

Introduction and objectives. The development of ablation techniques for supraventricular arrhythmias in patients with Ebstein's anomaly have led to a need for better understanding of the morphology of the triangle of Koch and the position of the atrioventricular (AV) node in this structure.

Methods. The study involved 17 human hearts: 11 with Ebstein's anomaly (age range: 37 weeks' gestation to 1 week after birth) and 6 structurally normal hearts (age range: 35 weeks' gestation to 2 days after birth). The area of the triangle of Koch was calculated and the length of the AV node and the bundle of His were measured.

Results. The area of the triangle of Koch was significantly smaller in specimens with Ebstein's anomaly than in control specimens (17.5±4.5 mm^2 vs. 25.5±6.5 mm^2; $P<.05$). The length of the AV node and its extensions were similar in hearts with Ebstein's anomaly and normal hearts. The AV node was displaced towards the base of the triangle in 73% of specimens with Ebstein's anomaly, and the inferior extensions reached the level of the cavotricuspid isthmus. In 91% of specimens with Ebstein's anomaly, the entry of the His bundle occurred before the apex of the triangle was reached and its length was shorter.

Conclusions. Morphologic findings in this study indicate that performing an ablation procedure close to the base of the triangle of Koch in patients with Ebstein's anomaly could result in AV nodal block.

Key words: *Atrioventricular node. Catheter ablation. Ebstein's anomaly.*

SEE EDITORIAL ON PAGES 633-4

El triángulo de Koch y el nodo AV en la anomalía de Ebstein: implicaciones en la ablación con catéter

Introducción y objetivos. Los avances realizados en los procedimientos de ablación de arritmias supraventriculares en la anomalía de Ebstein (AE) han creado la necesidad de un mejor entendimiento de la morfología del triángulo de Koch (TK) y disposición en dicha estructura del nodo auriculoventricular (AV).

Métodos. Se han estudiado 17 corazones humanos, 11 con AE (intervalo de edades, 37 semanas a 1 semana después de nacer) y 6 estructuralmente normales (intervalo de edades, 35 semanas a 2 días después de nacer). Se calculó el área del TK y se midió la longitud del nodo AV y el haz de His.

Resultados. El área del TK es significativamente más pequeña en los especímenes con AE que en los controles (17,5 ± 4,5 mm^2 frente a 25,5 ± 6,5 mm^2; $p < 0,05$). En los corazones con AE, el nodo AV y sus extensiones son similares en longitud a los corazones normales. El nodo AV en los especímenes con AE se desplaza hacia la base del triángulo en el 73% y las extensiones inferiores llegan al nivel del istmo cavotricuspídeo (ICT). En el 91% de los especímenes con AE, la entrada del haz de His se produce antes de llegar al ápex del triángulo, y su longitud es más corta.

Conclusiones. Con base en los hallazgos morfológicos obtenidos en este estudio, se puede deducir su utilidad en los procedimientos de ablación en las proximidades de la base del TK por la posibilidad de producir un bloqueo del nodo AV en pacientes con AE.

Palabras clave: *Nodo auriculoventricular. Ablación con catéter. Anomalía de Ebstein.*

This study was financed by the *Consejería de Infraestructuras y Desarrollo Tecnológico* (Regional Ministry of Infrastructure and Technological Development). *Junta de Extremadura* (Regional Government of Extremadura). [PRI 06B186 M.M and D.S.Q.] Spain.

Correspondence: Prof. D. Sánchez-Quintana.
Departamento de Anatomía y Biología Celular. Facultad de Medicina.
Universidad de Extremadura.
Avda. de Elvas, s/n. 06071 Badajoz. España.
E-mail: damians@unex.es; dasaqui55@yahoo.com

Received August 4, 2009
Accepted for publication February 2, 2010.

ABBREVIATIONS

AV: atrioventricular
CFB: central fibrous body
CSO: coronary sinus orifice
CTI: cavotricuspid isthmus
EA: Ebstein anomaly
TK: triangle of Koch

INTRODUCTION

Ebstein's anomaly (EA) is named after Dr Wilhelm Ebstein, who in 1866 described this congenital heart disease in detail after post-mortem examination of a 19-year-old patient.[1] Few morphological studies have been performed on the atrioventricular (AV) node in childhood and the node may change with age.[2-4] Previous studies in foetal hearts have shown that the AV node is located within Koch's triangle (KT) and closer to its base in EA compared with normal hearts.[5] Given the low incidence and wide spectrum of presentation of EA, there is no standardised ablation treatment for cases such as atrial flutter, AV nodal reentrant tachycardia, or accessory AV pathways, all of which have a morphological substrate in the vicinity of KT, with greater ablation complexity in paediatric patients.[6] Therefore, the objective of this study was to analyse the KT area and the conduction system arrangement (AV node and His bundle) in that structure in EA during the perinatal period.

METHODS

Seventeen formalin-preserved perinatal human hearts were studied, 11 with EA and 6 controls. We defined the perinatal period as being from 24 weeks of gestation to 28 days of life. The 11 specimens (6 males and 5 females) with EA belong to the collection of the Paediatrics Service of the Hospital Cruces de Baracaldo. Patients' ages ranged from 37 weeks to 1 week after birth and the heart weight at time of autopsy was 33.7 (6.4) g (range, 19-42.7 g). The 6 specimens structurally normal hearts were from 4 males and 2 females from 35 weeks of gestation to 2 days after birth. The weight of these hearts was 23.5 (4.5) g (range, 17-35 g). The study was approved by the University of Extremadura Ethics Committee.

For the KT dissection, the right atrium was opened from the tip of the atrial appendage to the AV junction along the right border of the heart. The incision was then extended to the right ventricle and superior vena cava. KT was exposed, inspected, and photographed to document the level of the AV junction. The dimensions of the sides of KT were taken using a ruler and quantitatively verified with calipers (Figure 1). The area was then calculated (area = b×h/2, where b = base; h = height of triangle). The transverse diameter of the coronary sinus orifice (CSO) and the tricuspid annulus were also measured using a string, the length of which was then measured with calipers.

Histological Study

The AV septal junction area was removed in block from each of the hearts. This area contains not only the borders of KT and adjacent parts of the interatrial and interventricular septum but also the superior area of the CSO. The blocks were dehydrated, embedded in paraffin, and serially sectioned at a thickness of 10 µm along an axis perpendicular to the tricuspid annulus. One out of every 10 sections was mounted and stained with Masson trichrome stain and van Gieson stain.

The lengths of the AV node and its extensions, as well as that of the His bundle, were calculated

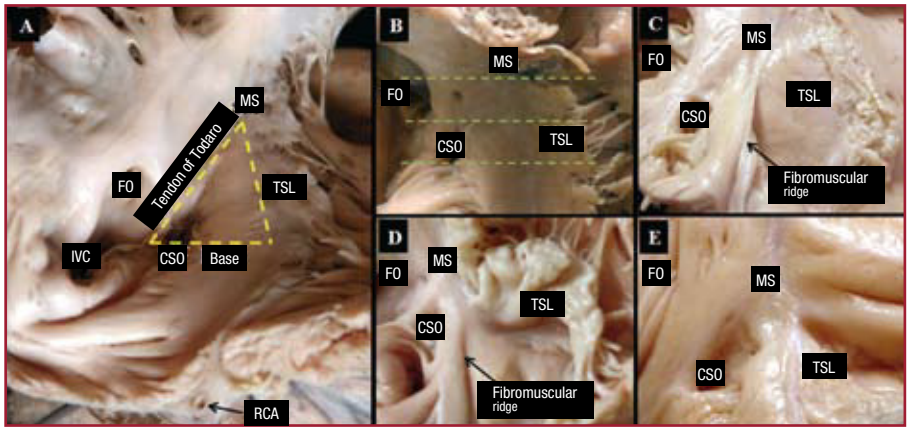

Figure 1. Koch's triangle in 2 control hearts (A and B) and 3 specimens with EA (C, D, and E). In panel B, 3 dashed green lines indicate 3 possible sections, one at the level of the base of Koch's triangle (coronary sinus orifice), another at the level of the mid-region of the triangle, and a third at the level of the apex (area of the His bundle). In the EA specimens, note the fibromuscular ridge in relation to the normal insertion of the septal leaflet of the tricuspid annulus (TSL) and the dysplasia of the leaflet. The smaller size of the triangle in those specimens with EA can be seen in photographs with similar magnification. CSO indicates coronary sinus orifice; FO, fossa ovalis; IVC, inferior vena cava; MS, membranous septum; RCA, right coronary artery.

TABLE 1. **Measurements of Koch's Triangle and its Area in Control Specimens and Those With Ebstein's Anomaly**

Koch's Triangle	Control	Ebstein's Anomaly	*P*
Base (side b), mm	6.1 (1.5) (range, 4-14)	4.6 (1.3) (range, 2-8)	
Tendon of Todaro (side a), mm	9.5 (2.6) (range, 4-17)	7.8 (1.4) (range, 3-12)	
Septal leaflet of the TV, mm	7.5 (1.5) (range, 5-13)	6.1 (1.3) (range, 4-9)	
Area of the triangle, mm^2	25.5 (6.5) (range, 16.3-34.5)	17.5 (4.5) (range, 12.3-27.5)	*P*<.05

TV indicates tricuspid valve.

from scanned histological sections using an image analysis programme (SigmaScan/Image Pro 5.0, Jandel Scientific, San Rafael, California, USA). The proportion of specialised myocytes to connective tissue in the body of the AV node was assessed on digital images at 40× magnification, onto which was placed a grid of 11 vertical and 11 horizontal lines, giving a total of 121 points of intersection on the grid. The intersection points where there was connective tissue were expressed as a percentage of connective tissue of the total 121 grid points (which is equal to 100%). Blood vessels and perivascular interstitial tissue were excluded from the quantification of connective tissue.

In order to gather more information on the structure and 3-dimensional organization of specialized cells in the AV node, His bundle, and the working and transitional atria, an ultrastructural study was conducted using scanning electron microscopy. For that study, slides or samples containing histological sections at least 20 µm thick were treated with 3 successive passes of 15 minutes in xylol to completely remove the paraffin in which they were embedded. These were dried at room temperature, placed on an aluminium support and put into a Bal-Tec SCD 005 vaporizer for 4 minutes, which produced a gold film, and then observed in a Jeol JSM-5600 scanning electron microscope.

Statistical Analysis

Results are expressed as mean (standard deviation). Quantitative results were compared using the Student *t*-test. A $P<.05$ was considered statistically significant.

RESULTS

Koch's Triangle in Control Specimens and Those With Ebstein's Anomaly

KT is located in the superficial paraseptal endocardium of the right atrium (Figure 1) with the insertion of the septal leaflet of the tricuspid valve as the anterior boundary. The tendon of Todaro forms the hypotenuse of the triangle and the base is formed by the CSO and the vestibule of the right atrium. The apex membranous septum is located in the area of intersection of the anterior and posterior borders of the triangle. In specimens with EA, there was an apical displacement of the septal leaflet towards the right ventricle, to which it is adherent. Therefore, the apex of the triangle was defined as the intersection of the tendon of Todaro with the true AV junction, which is marked in the majority of specimens by a fibromuscular ridge (7 specimens, 64%), or its remnant, since in the other 4 hearts it was a barely perceptible fibrous line. The length measurements of the various sides of the triangle and its area are shown in Table 1.

The tricuspid valve was malformed to varying degrees in all cases of EA, with significant expansion of the tricuspid valve annulus, 55.1 (10.7) mm (range, 43-75 mm) compared with controls, 28 (4) mm (range, 22-35 mm) ($P<.05$). The length of the sides and the area of the triangle was smaller in hearts with EA than in control hearts (17.5 [4.5] mm^2 vs 25.5 [6.5] mm^2; $P<.05$) (Table 1). Furthermore, the transverse diameter of the CSO was significantly higher in specimens with EA than in controls: 3.6 (1.2) mm (range, 1.5-7 mm) vs 2.2 [0.7] mm (range, 1.5-4 mm) ($P<.05$).

Atrioventricular Node and His Bundle in Control Specimens and Those With Ebstein's Anomaly

In all of the hearts, the body of the compact AV node was located within KT (Figure 2). In normal specimens, when the CSO was taken as a reference point in the histological sections, only the inferior extensions, and not the body, of the node reached the CSO. However, in most specimens with EA (8 hearts, 73%), given the smaller KT dimensions and greater diameter of the CSO, the body of the AV node ended up located at the level of the triangle base in relation to the CSO (Figure 2).

In control specimens, the body of the AV node had a semi-oval shape and was situated over the central fibrous body (CFB), the muscular AV septum was

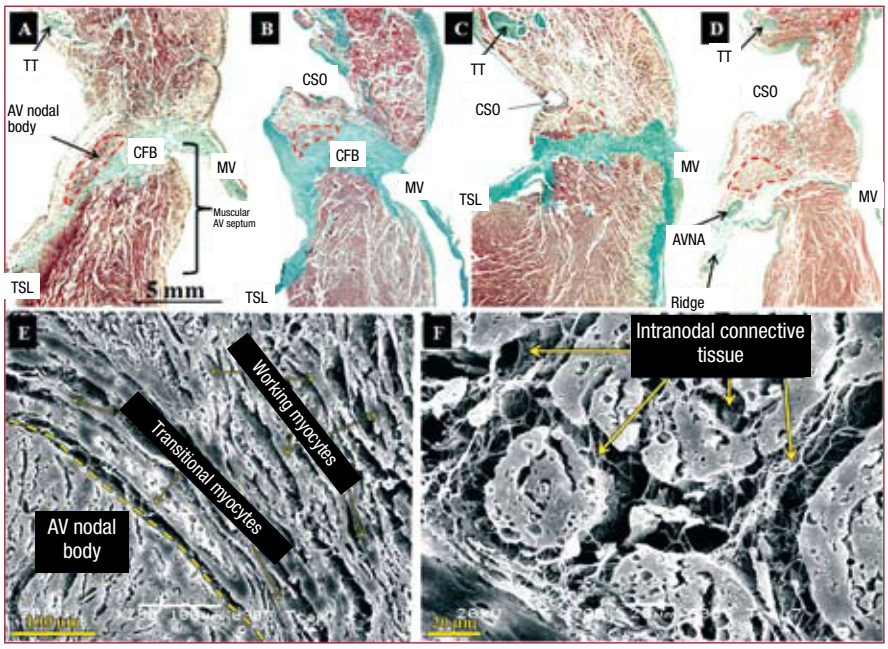

Figure 2. Sagittal histological sections (perpendicular to the tricuspid annulus) stained with Masson trichrome from a control heart (A) and 3 specimens with EA (B, C, and D) at the level of the body of the AV node (delimited with a dashed line red). Note how in the specimens with EA the body is at the level of coronary sinus orifice (CSO) and that the muscular AV septum (muscular area between the insertion of the tricuspid and mitral rings) is not appreciable and has a horizontal orientation. E and F are scanning electron microscopy images of a normal heart (E) and one with Ebstein's (F). Note the relationship of the AV node with the transitional myocytes and with the working atrial myocytes. The connective tissue matrix (mainly collagen) surrounds and is between the nodal cells. AVNA indicates AV nodal artery; CFB, central fibrous body; MV, mitral valve; TT, tendon of Todaro; TSL, tricuspid valve septal leaflet.

TABLE 2. **Measurements in mm of the Body of the Atrioventricular Node, Inferior Extensions, and His Bundle, in Control Specimens and Those With Ebstein's Anomaly**

	Control	Ebstein's Anomaly	*P*
Length of the compact body of the AV node, mm	1.6 (0.5) (range, 0.8-2.5)	1.7 (0.5) (range, 1.1-2.3)	≥.05
Length of the right inferior extension of the AV node, mm	0.5 (0.2) (range, 0.2-1.4)	0.6 (0.1) (range, 0.3-1.5)	≥.05
Length of the left inferior extension of the AV node, mm	0.4 (0.2) (range, 0-0.9)	0.5 (0.2) (range, 0-0.8)	≥.05
Length of the His bundle, mm	0.7 (0.2) (range, 0.3-1.2)	0.3 (0.2) (range, 0.2-0.7)	<.05

formed by the difference between insertion of the tricuspid and mitral rings in the interventricular septum, and the AV nodal artery was situated within the thickness of the node. In specimens with EA, the nodal body had a very irregular shape (semilunar, ovoid, comma, spindle) adapted to KT and the muscular AV septum, which is almost imperceptible in EA as shown in Figure 2B-D, so that the node is arranged almost horizontally on the central fibrous body (CFB) with a distance to the right atrial endocardium varying from 0.1 to 1 mm. In 3 EA specimens (27%), histological sections of the fibromuscular ridge showed the AV nodal artery passing in the thickness of the ridge in the direction of the node (Figure 2).

The body of the AV node extends from the beginning of the bifurcation of the node into its inferior extension to the beginning of the penetrating His bundle in the CFB. We found no significant differences in length of the body of the AV node between controls and specimens with EA. Its length, calculated from the histological sections in control specimens, was 1.5 (0.5) mm (range, 0.8-2.5 mm) and in specimens with EA was 1.7 (0.5) mm (range, 1.1-2.4 mm) (Table 2). The body of the AV node is made up of specialized myocytes (smaller in size than working myocytes), interlinked with one another without a particular orientation, surrounded by a matrix of connective tissue (Figure 2), and located between the CFB and a layer or more of transitional myocytes. Working atrial myocytes are located closer to the endocardium. A higher percentage of connective tissue enveloping the nodal cells was found in specimens with EA than in controls, 15.3% (2.3%) (range, 8%-22%) vs 8.7% (2.5%) (range, 4%-15%) ($P<.05$). The body of the AV node has inferior extensions. The right one runs toward the insertion of the septal leaflet of the tricuspid valve. The left one runs toward the CSO and mitral valve (Figure 3), although the right one was more common than the left (right 16 specimens, left 12). Its length can be seen in Table 2. We found no significant difference in length of the lower extensions between the controls and hearts with EA. However, the extensions did not extend past the base of KT at the level of the CSO in the controls, while in the EA specimens the right extension (7 specimens, 64%) was

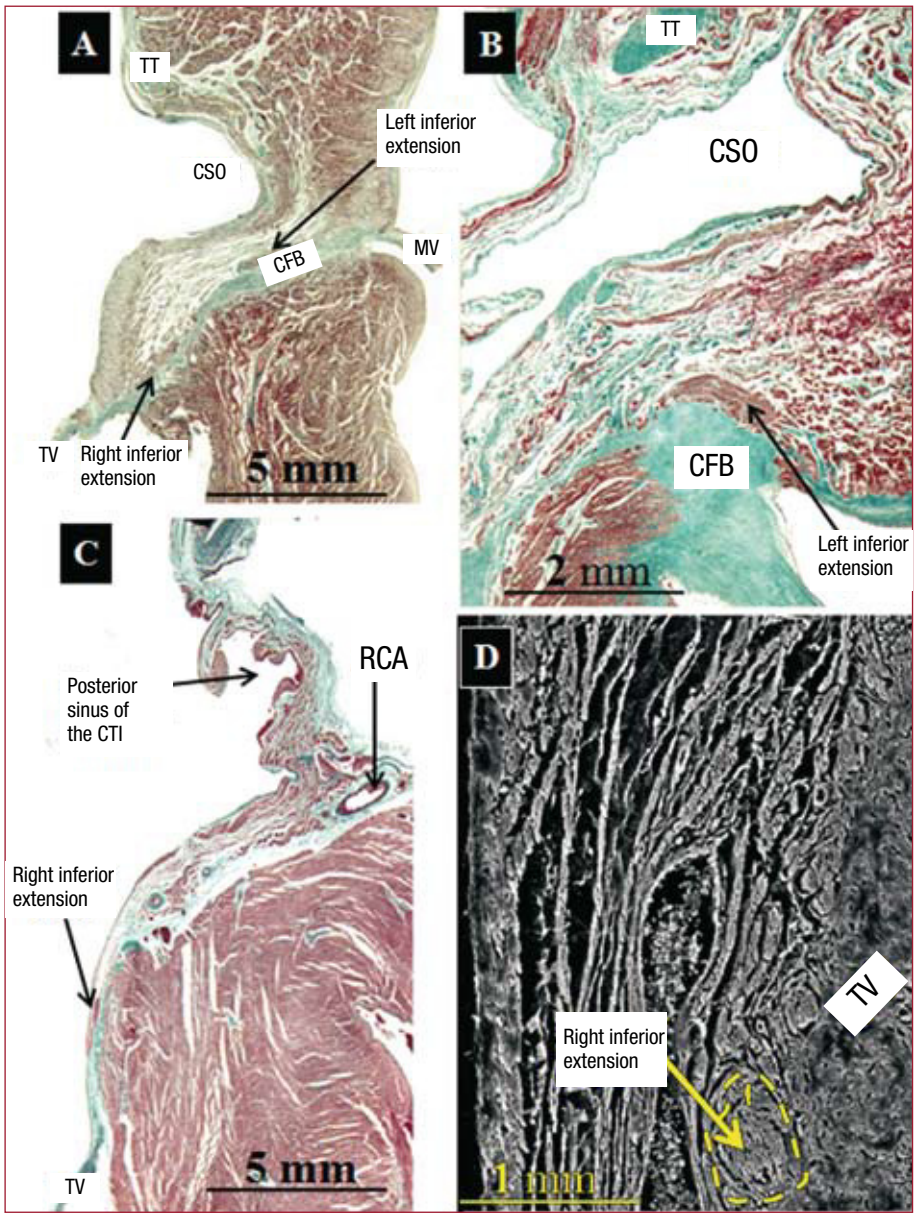

Figure 3. Sagittal histological sections stained with Masson trichrome from a control heart (A) and 2 with EA (B and C) at the level of the right and left inferior extensions from the body of the AV node. In A one can see how the right extension is oriented in relation to the septal leaflet of the tricuspid valve (TV) and the left in relation to the coronary sinus orifice (CSO). The left extension can be seen in B. In C the right extension is located at the same level of the posterior sinus of the cavo-tricuspid isthmus. D is a scanning electron micrograph of a right extension (next to the tricuspid valve) in a specimen with EA at the cavo-tricuspid isthmus. CFB indicates central fibrous body; MV, mitral valve; RCA, right coronary artery; TT, tendon of Todaro; TV, tricuspid valve.

lower, passing the base of KT to the level of the cavo-tricuspid isthmus (CTI) (Figure 3).

When the body of the AV node is oriented toward the apex of KT and enters the CFB, it is called the penetrating His bundle (Figure 4), which is electrically isolated (by connective tissue) from the rest of the atrial myocardium. The entry point is located in the area of intersection of the anterior and posterior borders of the triangle (membranous septum). In specimens with EA, the anterior border was defined as the fibromuscular ridge or its remnant that marks the true AV junction. Histologically, the beginning of the His bundle was found before reaching the apex in 50% of the control hearts (3 specimens) and in 91% (10 specimens) of those with EA (Figure 4). Furthermore, the His bundle was significantly shorter is length in cases of EA than in controls (Table 2).

DISCUSSION

Main Findings

Our study shows morphologically and quantitatively that KT is smaller in hearts with EA than in controls. The AV junction at the level of KT is marked by a fibromuscular ridge in the majority of specimens with EA. The body of the AV node and its extensions are shifted toward the base of KT and at the level of the CTI, respectively. Specimens with EA showed abnormal development of the muscular AV septum, since the insertion of the tricuspid and

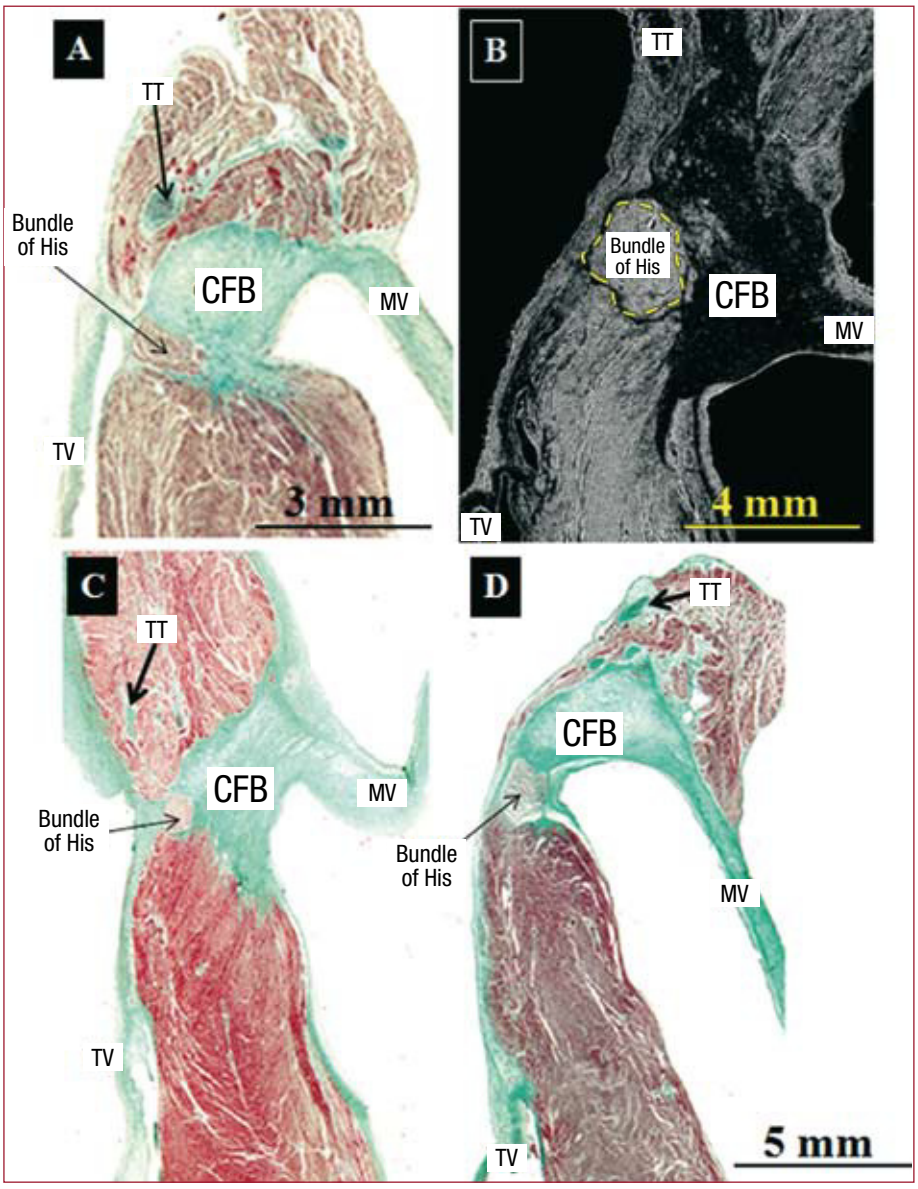

Figure 4. Sagittal histological sections stained with Masson trichrome (A, C, and D). Control hearts (A and B) and hearts with Ebstein's (C and D). B is a scanning electron micrograph of a control heart at the level of the penetrating His bundle. Except for image A where the His bundle crosses through the central fibrous body (CFB) at the apex of the triangle (junction of the septal leaflet of the tricuspid annulus with the CFB and tendon of Todaro), in the remaining images (B, C, and D), the His bundle crosses through the CFB before reaching the apex of the triangle. MV indicates mitral valve; TT, tendon of Todaro.

mitral valve rings are practically at the same height. Histologically, the entry point of the His bundle into the membranous septum occurred before reaching to the apex of KT in our cases with EA (91%, 10 specimens).

Koch's Triangle and the Atrioventricular Node in Specimens With Ebstein's Anomaly. Clinical Implications

Electrophysiologists recognize the potential risk of injuring the conduction system and consequently inducing AV block during catheter ablation in the area of KT and its anatomical surroundings, such as the CTI. The variability in the size and morphology of KT and the presence of the compact AV node and its extensions within its boundaries are essential anatomical determinants during the ablation procedure in paediatric patients.

The KT dimensions obtained in our study in normal hearts in the control group were similar to those previously described by Waki et al[4] in children under 1 year of age. However, KT was found to be smaller in hearts with EA, with 2 important anatomic findings, a larger CSO and the presence of an endocardial fibromuscular ridge marking the anterior boundary of the triangle. This ridge was described in adults by Cabrera et al[7] and later in foetuses by Ho et al.[5] The AV nodal artery runs through the thickness of this ridge in 27% of hearts with EA. The topography of the artery requires that the surgeon and/or electrophysiologist have precise knowledge to avoid injury when performing catheter ablation.

The body of the AV node and its extensions in

specimens with EA were similar in length to normal hearts and to those of children younger than 1 year.[4] In this sense, the smaller area of KT that occurs in EA implies a higher content of conduction tissue within its borders and a higher risk of injury to that tissue during catheter ablation. Furthermore, the reduced amount of space within KT could explain why the body of the AV node tends to move toward the base of KT in 73% of cases of hearts with EA. This shift is also seen in foetal hearts with EA,[5] although in that study the size of the triangle was not assessed.

In normal hearts approximately 1 year of age, the body of the AV node has been described as having a semi-oval shape in the muscular AV septum supported by the CFB, which has an oblique slope between the tricuspid and mitral valves.[4] In contrast to the control AV nodes, the shape of the nodal body in specimens with EA is very irregular (semilunar, ovoid, comma, spindle, etc.), adapting itself to the muscular AV septum, which, in contrast to control hearts, is not inclined but rather horizontal since there are no significant differences between the insertions of the tricuspid and mitral valve rings.

Our results show a significant increase in connective tissue surrounding and enveloping the body of the AV node in specimens with EA compared with controls. It is well known that the concentration of connective tissue increases during development and growth to maturity, or in pathological cases such as atrial fibrillation.[8] In our study, when dealing with specimens of similar ages, increased connective tissue in EA is explained by right heart failure due to dilatation of the tricuspid valve and right ventricular overload.

Inferior Extensions of the Atrioventricular Node. Clinical Implications

A relatively recent study by Inoue and Becker[9] reiterated what Tawara had described in 1906, that is, that the compact AV node has inferior extensions (right and left) and that these extensions, in 44% of adult hearts, may pass the coronary sinus orifice and reach the level of the sub-Eustachian sinus (posterior) of the CTI. A subsequent study[4] of structurally normal hearts showed that the extensions increased in length in relation to the age of the individual, but that the inferior extensions did not extend pass the CSO in hearts less than one year of age. Our study shows that in hearts with EA in the perinatal period, the inferior extensions, especially on the right (7 specimens, 64%) extend to the base of KT and lie at the level of CTI. It has been suggested that these extensions could provide an anatomical substrate for the so-called "slow pathway" in AV nodal reentrant tachycardia.[10]

Penetrating His Bundle: Apex of Koch's Triangle?

The AV node becomes the penetrating His bundle as we approach the apex of KT. The transition is marked by the entry into the CFB at its junction with the septal leaflet and the tendon of Todaro, both of which, as connective tissue, serve to electrically isolate the His bundle. Anatomically the penetrating His bundle is considered the apex of KT and coincides fluoroscopically with the area in which higher amplitude recordings are obtained on electrogram. However, our histological observations show that the entry point of the His bundle in the fibrous zone is usually prior to the apex of the triangle, especially in specimens with EA. This observation was previously described in some adult hearts, depending on a greater or lesser thickness of the CFB.[11] Variability in the position of the His bundle electrogram recording in relation to the KT borders as seen by right atrial angiography has been demonstrated in the electrophysiology laboratory.[12] Supporting our findings from control group postmortem hearts, the His bundle electrogram recording is not always at the apex of KT, defined by the anterosuperior border of the tricuspid valve annulus. Furthermore, in hearts with EA, the His bundle is significantly shorter in length than in controls. This could be because EA not only causes an abnormality in the development of the muscular AV septum but also of the CFB and its contents (His bundle). Future studies in the electrophysiology laboratory should correlate our anatomical findings with His bundle electrogram recordings in patients with EA.

Limitations of the Study

Collecting malformed hearts for histological study is currently difficult, especially when dealing with rare cardiomyopathies such as EA. Therefore, the majority of hearts with EA in this study were 25 or 30 years old. For all these years the hearts have remained fixed in formalin without observing any structural changes to the tissue. In hearts with EA, the morphologic spectrum of dysplasia of the septal leaflet is quite variable and is accompanied by associated cardiac malformations such as atrial septal defect and, at times, pulmonary valve stenosis or patent ductus arteriosus, although there was no mention of arrhythmias in the clinical records of the hearts with EA.

CONCLUSIONS

Knowledge of the dimensions of KT and the orientation of the AV node and its extensions in

EA may be clinically useful with in the setting of surgical treatment of the tricuspid valve and electrophysiological treatment of accessory pathways or other arrhythmic substrates near the base of KT, thus avoiding complications such as complete AV block.

REFERENCES

1. Ebstein W. Ueber einen sehr seltenen Fall von Insuffizienz der Valvula tricuspidalis, bedingt durch eine angeborene hochgradige Missbildung derselben. Arch fur Anat u Physiol. 1866:238–54.
2. James TN. Cardiac conduction system: Fetal and postnatal development. Am J Cardiol. 1970;25:213-26.
3. Becker AE, Anderson RH. Morphology of the human atrioventricular junctional area. In: Wellens HJ, Lie KT, Janse MJ, editores. The Conduction System of the Heart: Structure, Function and Clinical Implications. Lea & Febiger. Philadelphia; 1976. p. 263-86.
4. Waki K, Kim JS, Becker AE. Morphology of the human atyrioventricular node is age dependent: a feature of potential clinical significance. J Cardiovasc Electrophysiol. 2000;11:1144-51.
5. Ho S, Goltz D, McCarthy K, Cook AC, Connell MG, Smith A, et al. The atrioventricular junctions in Ebstein malformation. Heart. 2000;83:444-9.
6. Benito Bartolomé F, Sánchez Fernández-Bernal C. Ablación con catéter de vías accesorias en lactantes y niños de peso inferior a 10 kg. Rev Esp Cardiol. 1999;52:398-402.
7. Cabrera JA, Farré J, Sánchez-Quintana D, Rubio JM, Ho SY, Velasco D, et al. La unión aurículo-ventricular en la malformación de Ebstein de la válvula tricúspide: relevancia durante la ablación con catéter y radiofrecuencia. En Merino JL, editor. Problemas y desafíos en arritmias y electrofisiología cardíaca. St Jude Medical. Madrid; 2001. p. 201-18.
8. Hurlé J, Climent V, Sánchez-Quintana D. Sinus node structural changes in patients with long standing chronic atrial fibrillation. J Thorac Cardiovasc Surg. 2006;131:1394-5.
9. Inoue S, Becker AE. Posterior extensions of the human compact atrioventricular node: a neglected anatomic feature of potential clinical importance. Circulation. 1998;97:188-93.
10. Medkour D, Becker AE, Khalife K, Billete J. Anatomic and functional characteristics of a slow posterior AV nodal pathway: Role in dual-pathway physiology and reentry. Circulation. 1998;98:167-74.
11. Sánchez-Quintana D, Ho SY, Cabrera JA, Farre J, Anderson RH. Topographic anatomy of the inferior pyramidal space: Relevance to radiofrequency catheter ablation. J Cardiovasc Electrophysiol. 2001;12:210-7.
12. Farré J, Anderson RH, Cabrera JA, Sánchez-Quintana D, Rubio JM, Romero J, et al. Fluoroscopic cardiac anatomy for catheter ablation of tachycardia. Pacing Clin Electrophysiol. 2002;25:76-94.